WATER RESOURCES RESEARCH, VOL. 34, NO. 9, PAGES 2155–2168, SEPTEMBER 1998

Identification of large-scale hydraulic conductivity trends and the influence of trends on contaminant transport

Jack Eggleston and Stuart Rojstaczer
Center for Hydrologic Science, Duke University, Durham, North Carolina

Abstract. We examine the identification of large-scale spatial trends in hydraulic conductivity and the influence of these trends on contaminant transport. Using three different trend identification methods, polynomial regression and Kalman filtering, which fit smooth functions, and hydrofacies delineation, which constructs a geologic model, we try to identify the hydraulic conductivi ± ty patterns controlling solute transport in a heavily sampled heterogeneous aquifer on Columbus Air Force Base, Mississippi. Even with >2400 hydraulic conductivity measurements, unambiguous determination of large-scale trends is not possible. None of the estimated hydraulic conductivity trends gives transport simulations that reproduce the observed non-Gaussian transport behavior. Hydrofacies delineation and Kalman filtering give the best results. While the influence of the identified large-scale trends on advective transport is significant, accurate prediction of contaminant transport requires knowledge of small-scale (<10 m) hydraulic conductivity structures.

1. Introduction

The spatial heterogeneity of hydrogeologic parameters, particularly hydraulic conductivity, makes prediction of groundwater flow and contaminant transport difficult. Hydraulic conductivity, the primary hydrogeologic parameter controlling transport, is highly variable in most alluvial aquifers, varying at some sites by 6 orders of magnitude over a distance of <10 m. Before groundwater flow and contaminant transport can be modeled in detail a three-dimensional map of hydraulic conductivity and other key hydrologic parameters is needed. Obtaining measurements of the subsurface is an involved, expensive process, and the limited resources of any groundwater investigation allow only an incomplete picture of the subsurface. Investigators therefore must interpolate sparse spatial data to build models of groundwater systems.

A common approach for modeling subsurface transport is to assume that hydraulic conductivity K variations on a large spatial scale control advective transport and hydraulic conductivity variations on a small spatial scale control dispersive transport [*Scheibe and Cole*, 1994]. The exact definitions of "large-scale" and "small-scale" can vary depending on the density of measured data and the amount of natural heterogeneity present. Although some studies assume that hydraulic conductivity varies on two scales, large and small [*Rajaram and McLaughlin*, 1990; *Brannan and Haselow*, 1993], others assume that it varies on multiple scales [*Dagan*, 1986; *Cushman*, 1990, chap. 1) or on a continuous hierarchy of scales [*Neuman*, 1990]. In the terminology of geostatistics, hydraulic conductivity variations that have a spatial scale large enough to be described in at least a roughly deterministic manner are known as a "trends" or "drift" and smaller-scale variations, which can only be described statistically because of the sparsity of data, are known as "residuals."

It is generally assumed that large-scale hydraulic conductivity trends control the bulk movement of groundwater and associated contaminants. Attempts to predict bulk flow patterns and solute transport therefore require knowledge of hydraulic conductivity trends. Because variations in flow velocity are the dominant mechanism for field-scale solute dispersion [*Güven et al.*, 1984], hydraulic conductivity trends must also be identified before solute dispersion can be understood. The stochastic equations of *Gelhar and Axness* [1983] and *Dagan* (1982), which predict field-scale dispersion as functions of ln (K) variance and ln (K) correlation lengths, require a geostatistically homogeneous flow field and hydraulic conductivity correlation scales that are small compared to the scale of transport. Before these stochastic equations can be applied to predict transport, nonstationary hydraulic conductivity patterns (trends) must be identified and removed.

Separating fluctuations in hydraulic conductivity according to spatial scale is not a straightforward process. Variograms and related second-order statistics that express scale dependent variation are not able to indicate the form of large-scale trends and sometimes do not even indicate their presence [*Russo and Jury*, 1987a, b]. Although the presence of trends will generally increase the sill (variance) and correlation length of the variogram, the form of trends cannot be deduced from variograms.

In this study we examine our ability to accurately describe large-scale spatial variations in hydraulic conductivity found in a heterogeneous alluvial aquifer. Perhaps more importantly, we examine the influence of the inferred large-scale trends on solute transport. The site we have chosen for this study is one of the most hydrogeologically characterized heterogeneous aquifers in the world; the alluvial sediment aquifer at Columbus Air Force Base, Mississippi [*Boggs et al.*, 1990].

The first approach we use to determine spatial trends is that of traditional geostatistics, which treats hydraulic conductivity as a correlated random field and assumes that nonstationary variations or trends follow a continuous function, usually a linear function or low-order polynomial. The second approach is to assume that large-scale spatial variation of subsurface hydrologic variables is controlled by geologic architecture and to assign hydraulic conductivity according to position within

Paper number 98WR01475.
0043-1397/98/98WR-01475$09.00

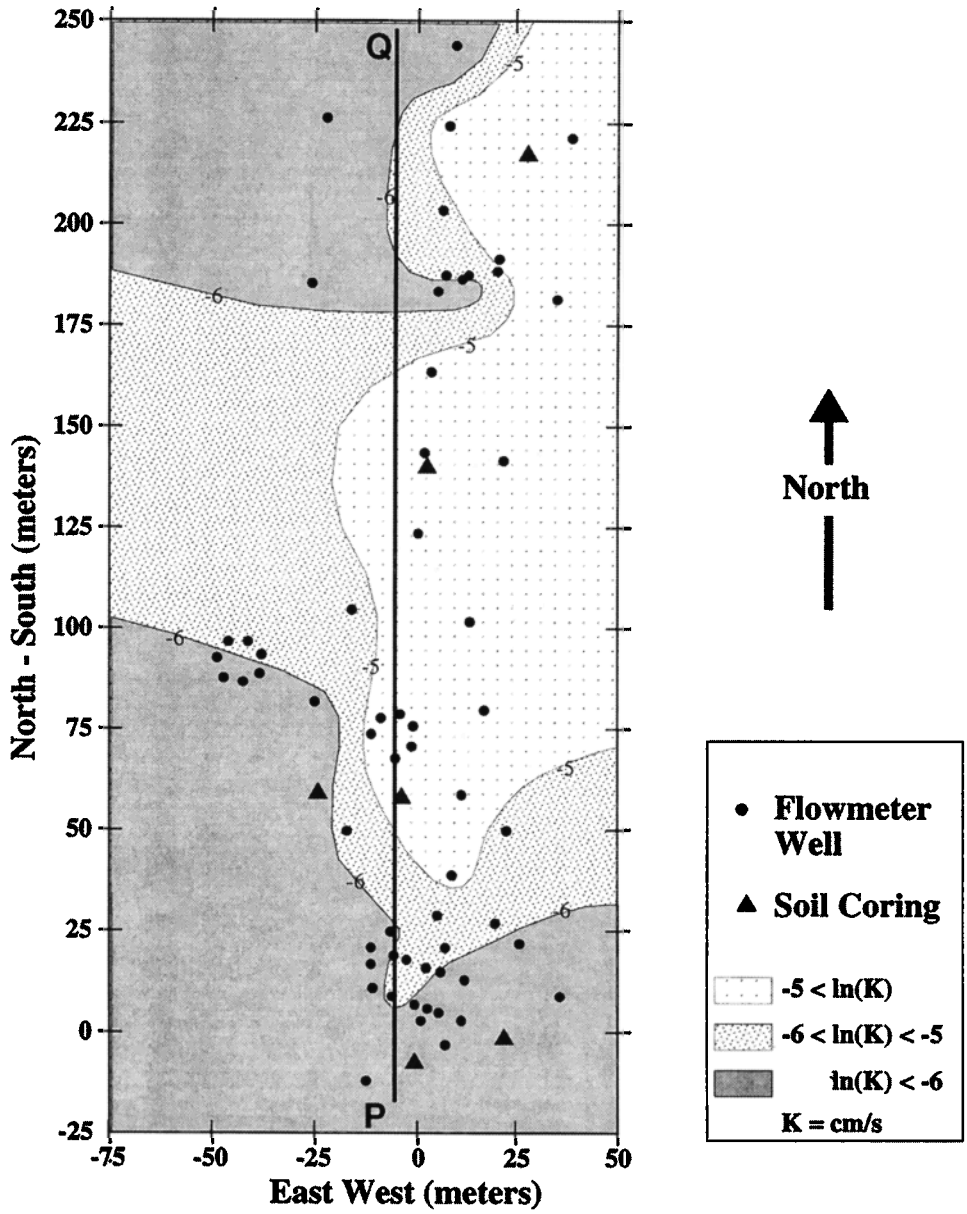

Figure 1. Location of wells (circles) and cores (triangles) on Columbus Air Force Base. Shading indicates vertically averaged ln (K), where K is in cm s^{-1}. Higher K is more lightly shaded.

the assemblage of geologic units [*Fogg*, 1986; *Webb and Anderson*, 1996; *Scheibe and Freyberg*, 1995]. We assess the relative worth of these two approaches by examining the relative ability of the inferred hydraulic conductivity to be used as a means of predicting solute transport at Columbus Air Force Base.

Previous work at Columbus Air Force Base has examined the ability of stochastic theories to predict dispersive transport of tracers [*Adams and Gelhar*, 1992; *Rehfeldt et al.*, 1992]. A major conclusion was that nonstationary patterns in the hydraulic conductivity and hydraulic head fields violate the requirements of stochastic dispersion theories. Various methods were then used to filter out the large-scale hydraulic conductivity trends so that the stochastic theories could be applied to the residuals or small-scale hydraulic conductivity variations. The results of these studies left questions about what defines a trend and how well a least squares method can determine a trend from available measured data. In contrast, this study focuses on methods of trend identification and investigates the relation between large-scale hydraulic conductivity trends and bulk contaminant transport at Columbus Air Force Base.

2. Site Description

The field data used in this study are from the aquifer test site at Columbus Air Force Base, Mississippi. Extensive flowmeter measurements of hydraulic conductivity and sediment core samples taken at the site have been published previously and are available for study [*Boggs et al.*, 1990; *Rehfeldt et al.*, 1992]. Locations of test wells and sediment cores are shown in Figure 1. The aquifer at the test site is a shallow (<15 m depth) sand and gravel braided stream Pleistocene deposit, probably associated with the nearby Tombigbee and Buttahachee Rivers. Several meters of silt and clay form the unsaturated zone overlying the sand and gravel aquifer. The Eutaw formation, a

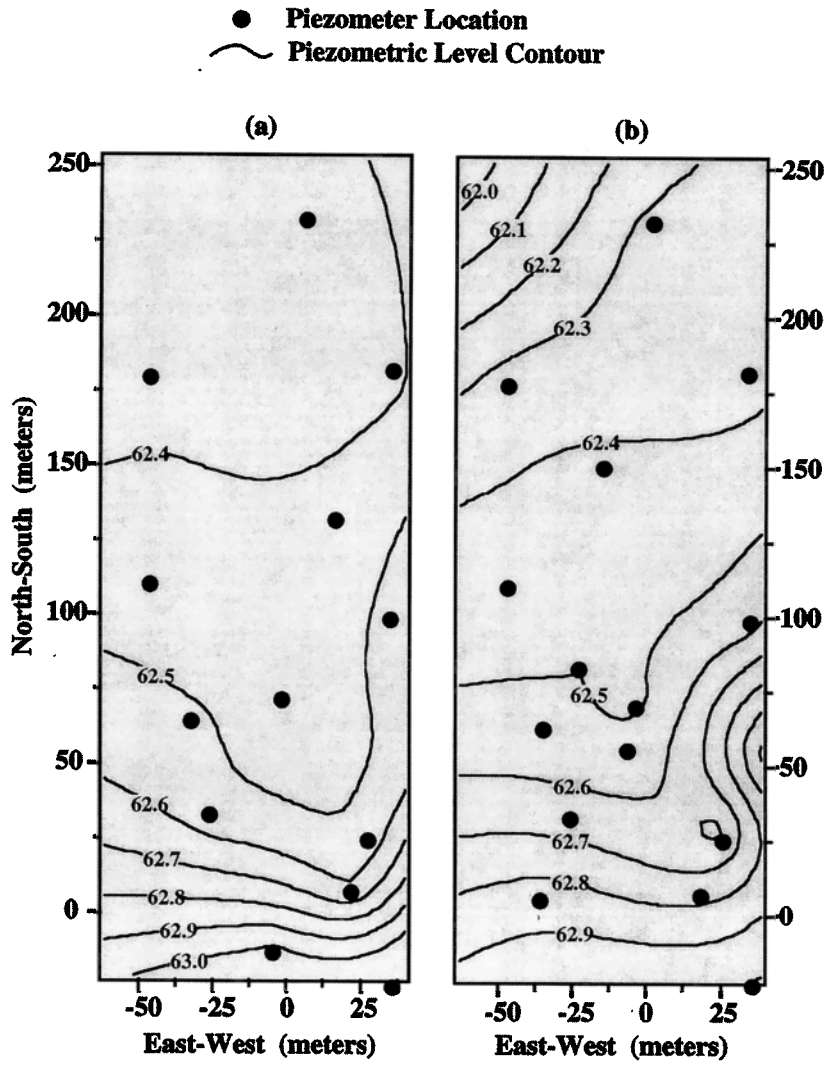

Figure 2. Piezometric levels (m mean sea level (msl)) on October 11, 1989, interpreted from monitoring wells (circles): (a) wells screened above 58 m MSL and (b) wells screened below 58 m.

silt and fine sand Cretaceous marine deposit [*Mallory*, 1993], underlies the sand and gravel unit and is assumed to act as a relatively impermeable basement unit.

Mean ln (K) calculated from 2451 flowmeter measurements is -5.4, with K in cm s^{-1}. The aquifer is heterogeneous, exhibiting textural variations from the centimeter to the 100 m scale. The ln (K) variance of 4.4 is high as compared to a value of 0.38 for the Borden aquifer [*Sudicky*, 1986] and 0.24 for the Cape Cod aquifer [*Hess et al.*, 1992]. The degree of data density can be gauged from the number of measurements per integral volume, ~2, which is low compared to the 30 measurements per integral volume at the much less heterogeneous Cape Cod site [*Eggleston et al.*, 1996]. Several natural gradient tracer tests have been performed at the Columbus Air Force Base site. We use the results of a bromide test performed between October 1986 and June 1988 [*Adams and Gelhar*, 1992] as a basis for transport simulations.

Experimental evidence indicates the presence of large-scale trends in hydraulic conductivity at the Columbus Air Force Base site. The piezometric levels in Figure 2 show flow converging to the center of the well field, most likely because of a region of higher hydraulic conductivity in the central field. A further indication of a region of high hydraulic conductivity is that spacing between head contours is greater in the central region than in the southern region of the well field. The behavior of the injected bromide plume also gives evidence of a nonstationary hydraulic conductivity field. During the tracer experiment a 10.07 m^3 slug of solute with a bromide concentration of 2500 mg L^{-1} was injected into the aquifer and allowed to migrate under natural gradient conditions. At elapsed times of 9, 49, 126, 202, 279, 370, and 503 days, groundwater samples were drawn from an extensive network of multilevel wells and analyzed. The behavior of the plume indicates a heterogeneous, nonstationary flow field. In Figure 3 it can be seen that after 503 days the peak concentration of bromide has moved <10 m whereas dilute bromide concentrations reached the sampling well farthest downgradient, 170 m from the injection well.

Direct evidence of both vertical and horizontal large-scale hydraulic conductivity trends is given by flowmeter measurements of hydraulic conductivity. Figure 4 shows hydraulic conductivity along a vertical section aligned with the principal direction of groundwater flow. A region of higher ln (K) can be seen between 75 and 200 m N–S, above an elevation of ~57

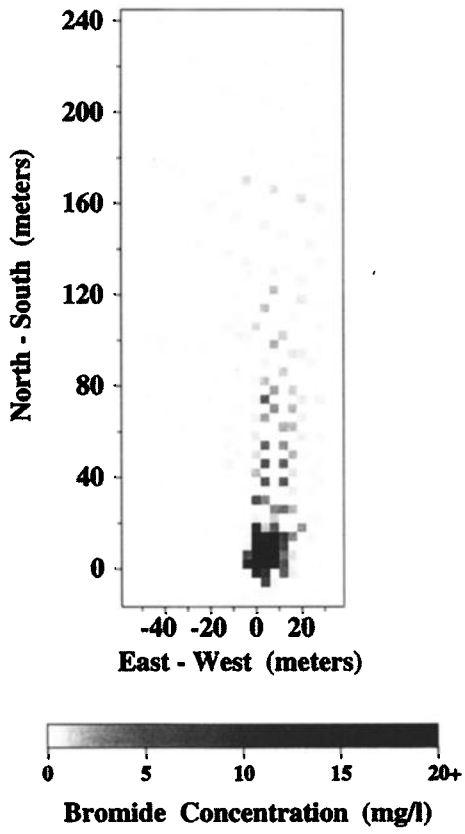

Figure 3. Observed depth-maximum bromide concentrations at 503 days of transport. Darker shading indicates higher observed concentration. Note the non-Gaussian plume behavior.

m. This region is shown in the plan view as the lightly shaded area of Figure 1.

Vertical trends in hydraulic conductivity are also suggested by changing sediment texture with depth. The locations of the six cores considered here are shown in Figure 2. Grain size analyses were performed on segments of each core at ~1.5 m vertical intervals [*Boggs et al.*, 1990]. The 10% grain size (d_{10}), often assumed to be proportional to the square root of hydraulic conductivity, is shown as a function of elevation in Figure 5. A decrease in the d_{10} grain size is seen below an elevation of 57 m mean sea level (msl), indicating that hydraulic conductivity most likely also decreases below this elevation. Using the proportionality between d_{10}^2 and hydraulic conductivity, a ratio between average hydraulic conductivity above and below 57 m MSL is predicted to be 25.0.

$$K \approx d_{10}^2 \tag{1}$$

$$K_{\text{upper}}/K_{\text{lower}} = \frac{(d_{10_{\text{upper}}})^2}{(d_{10_{\text{lower}}})^2} = \frac{(0.6)^2}{(0.12)^2} = 25 \tag{2}$$

3. Trend Estimation Methods

Because the true hydraulic conductivity field is unknown, except for scattered local measurements, large-scale trend values must be estimated. In the hydrologic literature, there is no consensus on the best approach for identifying large-scale trends. This uncertainty is due perhaps to wide variability in aquifer conditions and the lack of extensive field data for evaluating different methods. More likely, the uncertainty is due to the inherent difficulty of defining the difference between small-scale and large-scale spatial variations.

We used three different methods to estimate the large-scale hydraulic conductivity trend at Columbus Air Force Base and evaluated the methods by comparing transport modeling results to field tracer tests. The three methods we used to estimate the large-scale trends are (1) polynomial regression, (2) distributed parameter Kalman filtering, and (3) hydrofacies delineation. All three methods use hydraulic conductivity measurements taken with the downhole flowmeter as the basis of estimation. Hydrofacies delineation also incorporates sediment core information. All trend estimation is performed in ln (K) space. The inverse natural log of the estimated trend values are then taken to transform back to K space for trend comparison and transport simulation. Each method is discussed separately below.

3.1. Polynomial Regression

A spatial trend can be estimated by fitting a polynomial regression model to the data. The order of the polynomial and the number of terms must be specified on the basis of the available knowledge of the variable. Because higher-order trends have more parameters, allowing more inflections and variations in the polynomial trend field, higher-order polynomials generally account for more of the observed variance. As the trend order increases, smaller-scale variations are captured by the polynomial, so subjective judgment must be used to decide what trend form is most appropriate. The problem of choosing a polynomial form for the trend model is often difficult to resolve. In general, it is not possible to determine the actual trend from experimental variograms. One must instead make a judgment based on supplementary data or knowledge of the phenomenon. Previous studies have analyzed flowmeter data from the Columbus Air Force Base site and arrived at different conclusions about what polynomial form is best. *Rehfeldt et al.* [1989] analyzed 1242 of the flowmeter K measurements and, after fitting polynomials from order 1 to 3, decided that a second-order trend best fit the data. The third-order trend was rejected because it was found to be incompatible with tracer data. *Young et al.* [1990] analyzed 881 K values and, after examining polynomial expressions from orders 1 to 6, concluded that the best polynomial form for describing the trend could not be determined and that polynomial expressions were not well suited for describing the hydraulic conductivity patterns at Columbus Air Force Base. *Rehfeldt et al.* [1992] analyzed 2187 of the flowmeter measurements and, primarily on the basis of tracer data, decided that a third-order polynomial could best describe trend behavior.

We use the same third-order polynomial form as *Rehfeldt et al.* [1992]:

$$\ln(\hat{K}) = \sum_{j=1}^{N} a_j F_j(x_i) \tag{3}$$

$$\begin{aligned}\ln(\hat{K}) = {} & a_0 + a_1X + a_2Y + a_3Z + a_4XX + a_5XY + a_6XZ \\ & + a_7YY + a_8YZ + a_9ZZ + a_{10}XXX + a_{11}XXY \\ & + a_{12}XXZ + a_{13}XYY + a_{14}XYZ + a_{15}XZZ \\ & + a_{16}YYY + a_{17}YYZ + a_{18}YZZ + a_{19}ZZZ\end{aligned} \tag{4}$$

where ln ($\hat{K}$) is the estimated trend component of the natural logarithm of hydraulic conductivity, x_i are data coordinate

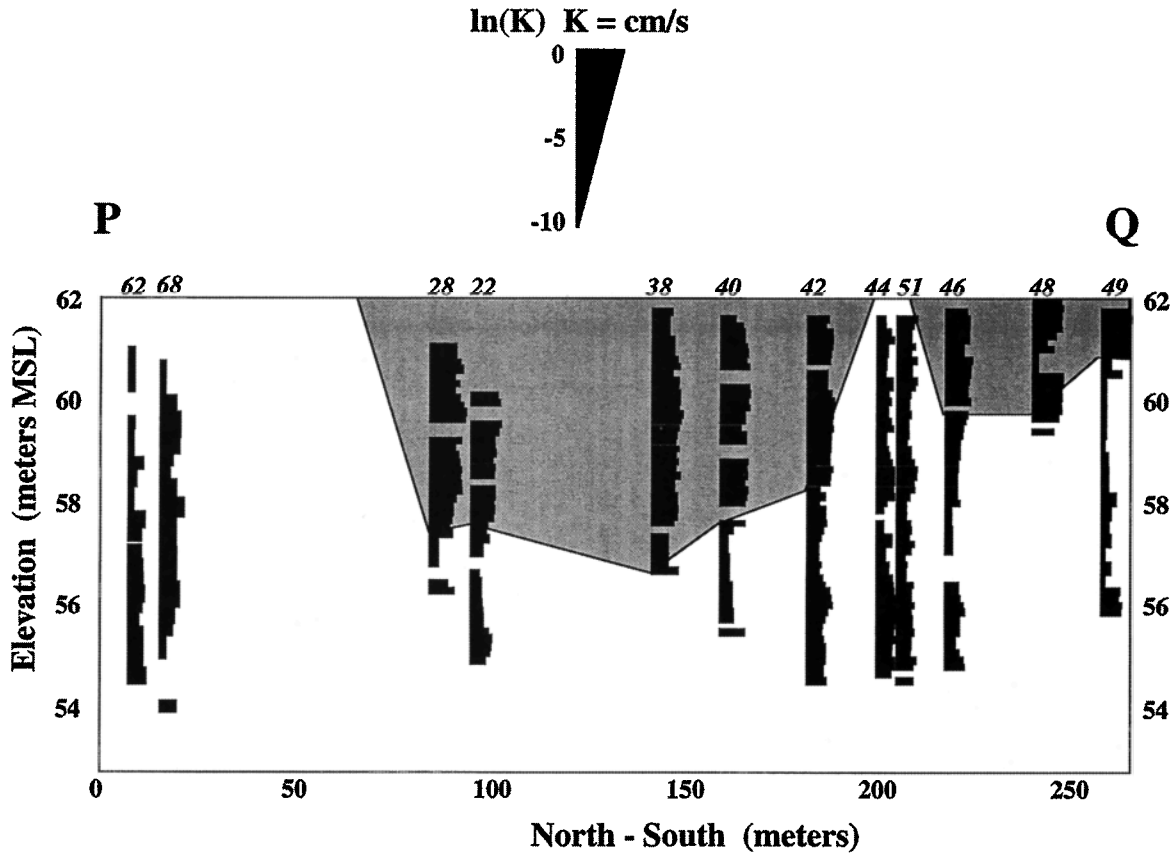

Figure 4. Measured hydraulic conductivity along vertical section PQ, the mean direction of flow. Each vertical black bar represents one flowmeter well. Wider bars indicate higher hydraulic conductivity (cm s^{-1}), and the lowest elevation of each stack is where flowmeter testing was discontinued. The shaded area indicates the coarser sediment region from the hydrofacies delineation procedure.

locations (i = 1, 2, and 3), $F_i(x_i)$ are functions of coordinate values, and a_i are the regression coefficients. Ordinary least squares (OLS) regression is performed to determine the regression coefficients. *Russo and Jury* [1987a] found that OLS was as accurate as more complicated regression methods in determining a trend. Following *Boggs et al.* [1990], weights given by (5) are used in the regression to account for expected measurement error.

$$W(x) = K_x^{0.25} \tag{5}$$

Because we use a slightly larger set of flowmeter measurements, 2451 versus 2187, and use OLS rather than multiple linear regression, our regression coefficient values (a_i) are different than those obtained by *Rehfeldt et al.* [1992]. One disadvantage of the polynomial trend modeling is that there is no direct way to control the spatial scale of the variations captured by the polynomial; the scale depends on the form of the polynomial, data locations, and data values.

3.2. Kalman Filtering

A distributed parameter Kalman filter can also be used to estimate a large-scale trend in irregularly spaced spatial data. *Rajaram and McLaughlin* [1990] present such a method and demonstrate it using a subset of two-dimensional hydraulic conductivity data from the Columbus Air Force Base site. The method assumes that spatial variability occurs on two scales: a large scale (the trend) and a small scale (random deviations). Large- and small-scale signals are captured with linear filters

$$\hat{m}(x) = K_m(x)Z \tag{6}$$

$$\hat{l}(x) = K_l(x)Z \tag{7}$$

where Z are the observed data, $\hat{m}(x)$ and $\hat{l}(x)$ are the esti-

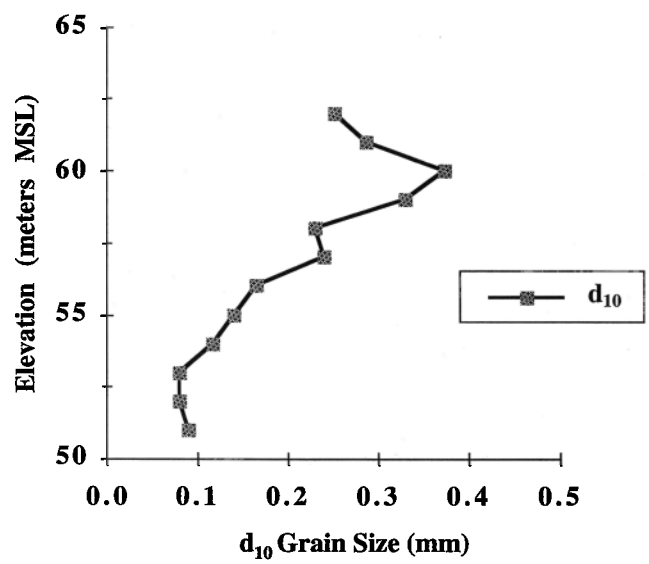

Figure 5. The d_{10} grain size (millimeters) with depth. The average of the six cores is given in Figure 1. The average value at 57 m excludes an outlier d_{10} value of 5.0 mm.

mated large- and small-scale signal values, and $K_m(x)$ and $K_l(x)$ are weights for the large- and small-scale signals at location x. A spatial covariance model must be assumed for the large-scale signal and for the small-scale signal, and it is further assumed that the two signals are independent, with a zero cross covariance at all lags. The linear filter weights are calculated using the covariance models

$$K_m(x)P_{ZZ} = P_{mm}(x - x_j) \tag{8}$$

$$K_l(x)P_{ZZ} = P_{ll}(x - x_j) \tag{9}$$

where P_{ZZ} is an $N \times N$ covariance matrix for the measured data with N equal to the number of measurements, P_{mm} and P_{ll} are $1 \times N$ covariance vectors for the large- and small-scale signals at location x, x_i, and x_j are measurement locations, and i and j are values from 1 to N. More details on the method are given by *Rajaram and McLaughlin* [1990].

A major drawback of distributed parameter Kalman filtering is that the covariance form, variances, and correlation lengths must all be assumed for both large- and small-scale signals. The choice of covariance parameters strongly affects the resulting estimated fields and consequently affects any transport modeling based on the estimated fields [*Rajaram and McLaughlin*, 1990]. Complicating this is the problem of having no straightforward way to a priori determine the covariance parameters because observations are a combination of the large- and small-scale signals.

We follow the common practice in stochastic hydrology of using a negative exponential function to model ln (K) covariance

$$P(h) = \sigma_Z^2 \exp\left[-\left(\frac{h_i^2}{\lambda_i^2}\right)^{1/2}\right] \tag{10}$$

where $P(h)$ is the covariance for separation distance h, σ_Z^2 is the variance, h_i is the separation vector, and λ_i is the correlation length vector (with $i = 1$, 2, and 3). Looking to the scale of patterns in Figures 1–4, we assume a horizontal correlation length of 150 m for the large-scale trend. We assume a horizontal correlation length of 1.5 m for the small-scale signal. For both large- and small-scale covariance models we assume the vertical correlation length to be 12.5% of the horizontal correlation length, and we attribute half of the total measured variance (50% of 4.4 = 2.2) to each signal. In distinguishing between covariance parameters for the large- and small-scale signals we had little objective information to guide us and settled on the above parameters because the resulting estimated field captured the large-scale trends reasonably well on the basis of visual comparison to the measured field. If different covariance parameters were assumed, the hydraulic conductivity field estimated by the Kalman filter would change, and the transport results based on the estimated hydraulic conductivity values would also change.

3.3. Hydrofacies Delineation

An alternate approach to estimating large-scale spatial trends for hydrologic variables is to estimate the geologic architecture of the depositional units making up the aquifer and then to assign hydrologic parameter values according to depositional unit. This approach is commonly used in the description of petroleum reservoirs [*Weber*, 1986] and has seen increasing attention in hydrology (see *Koltermann and Gorelick* [1996] for a review). A usual assumption of the approach is that sediment facies type controls hydrologic parameter values. Within each geologic unit, there may be local heterogeneity or small-scale variations, but the primary variation in hydraulic parameters is generally assumed to exist across geologic units.

We apply a simple two-component form of this geologic architecture approach to estimate large-scale hydraulic conductivity trends at the Columbus Air Force Base site. On the basis of the hydrologic and sedimentary evidence presented in the previous section we separate one region of predominantly coarse sediments from a surrounding region of predominantly fine sediments. The region of predominantly high K sediments in the middle of the test site possibly corresponds to an abandoned river meander subsequently filled with sands and gravels. Previous investigators have attempted to delineate boundaries of the supposed river channel at Columbus Air Force Base. *Young et al.* [1990] divide the aquifer into regions, with an elevation of 58.5 m marking a boundary between the bottom of the river meander and the top of the braided stream deposits. *Rehfeldt et al.* [1992] place this same boundary at an elevation of 57.5 m on the basis of vertical grain size trends seen in sediment cores.

Flowmeter hydraulic conductivity measurements from the 60 wells and particle size analyses from the six sediment cores (Figure 1) are used to define the boundaries of the high hydraulic conductivity region. The sediment cores show finer sediment texture with increasing depth (Figure 5), suggesting separate hydrofacies in the upper and lower aquifer. A moving average of flowmeter ln (K) is taken for each well using a 2 m vertical averaging window. A cutoff level of ln (K) = -5.1 is used to divide the vertically averaged measurements between high and low K regions in each well. Averaged ln (K) values >-5.1 are considered to be located in a sandy gravel unit with higher hydraulic conductivity, while averaged ln (K) values <-5.1 are considered to be located in a clayey sand unit having lower hydraulic conductivity. At each well having averaged ln (K) values above -5.1 a single elevation corresponding to ln (K) = -5.1 is sufficient to divide high ln (K) measurements from low ln (K) measurements.

After positioning the sediment unit boundaries we assume that hydraulic conductivity is constant within each hydrofacies and equal to the mean of the flowmeter measurements. The high data density at the Columbus Air Force Base site could allow more detailed modeling of geologic architecture than the two-zone model that we apply. For example, in a study using inverse modeling to examine major heterogeneities at Columbus Air Force Base, *Hill et al.* [1996] used multiple hydrofacies zones to assign hydraulic conductivity values. It is also possible to define separate covariances for each sediment unit, particularly for the regions with high flowmeter well density. However, as the complexity of the geologic model increases, a lack of sufficient data makes decisions about the positions of geologic units and spatial variation within the units increasingly arbitrary and subjective. Because we are interested in the largest-scale variations, we take a conservative approach in creating the hydrofacies model and only use two hydrofacies.

4. Results of Hydraulic Conductivity Trend Identification

Each of the trend estimation methods, polynomial regression, Kalman filtering, and hydrofacies delineation, produces a three-dimensional field of hydraulic conductivity values. For comparison to the estimated trend fields we also consider a

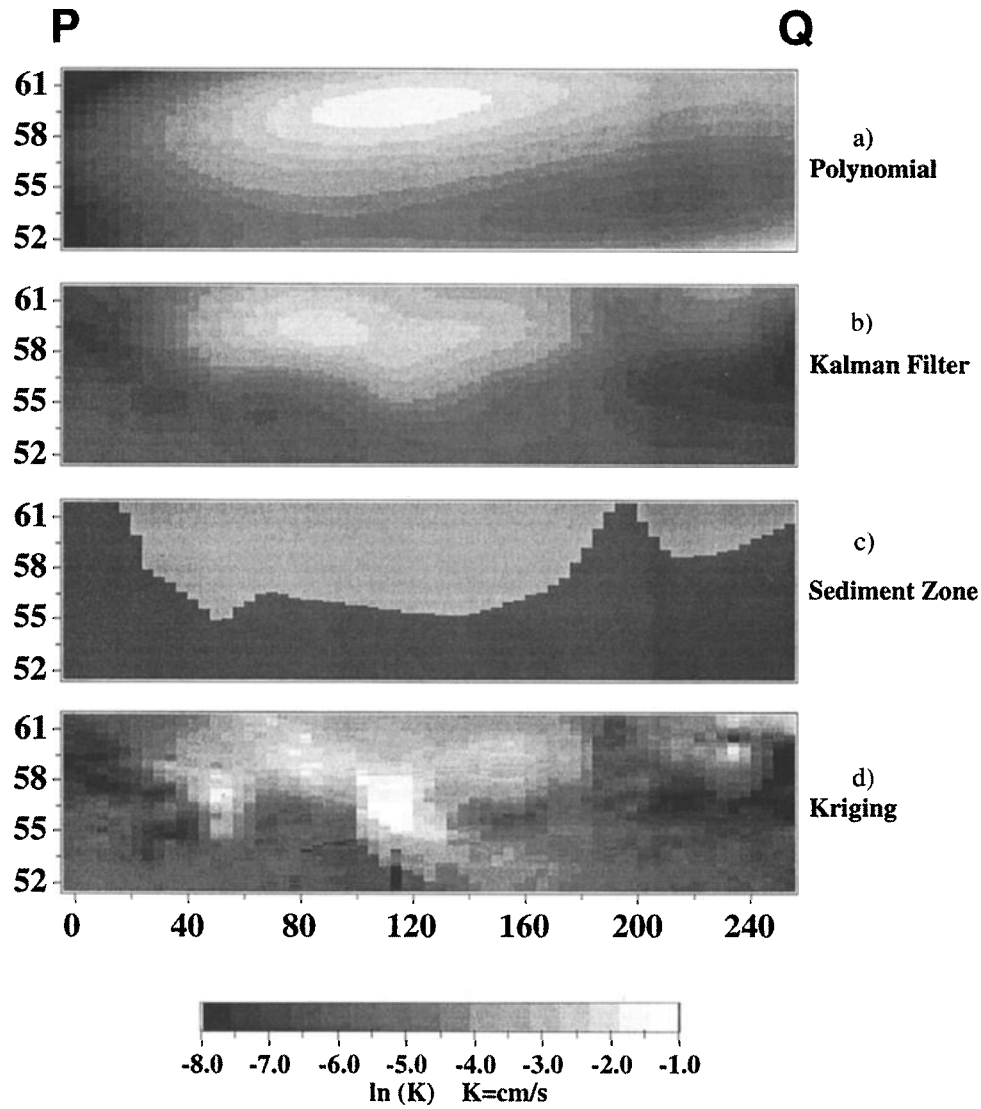

Figure 6. Hydraulic conductivity values, vertical section PQ: (a) polynomial regression trend, (b) Kalman filter trend, (c) hydrofacies trend, and (d) Kriged values. Lighter shading indicates higher hydraulic conductivity.

field of hydraulic conductivity values produced by ordinary kriging, which accounts for more small-scale hydraulic conductivity variation than any of the trend estimation methods. Vertical sections showing hydraulic conductivity trend values along the direction of flow are given in Figures 6a–6d. Horizontal sections approximately through the middle of the bromide plume region showing hydraulic conductivity trend values are given in Figures 7a–7d. All three trend estimation methods produce trend fields that show hydraulic conductivity increasing with elevation and increasing from west to east. Experimental variograms for the trend ln (K) values are shown in Figures 8a–8b. The experimental variograms for all three trend fields show lower sills and longer correlation than the measured ln (K) values, as is expected (Table 1). The estimated hydraulic conductivity trends are discussed separately for each method below.

4.1. Polynomial Regression

Polynomial regression produces an estimated hydraulic conductivity trend field with less small-scale variation than either Kalman filtering or hydrofacies delineation (Figures 6 and 7). However, the large-scale trends in the polynomial field are strong and cause the polynomial trend field to have the largest variance and longest spatial correlation length of the three methods. The trend ln (K) variance of 3.1 indicates that the regressed polynomial accounts for ~70% of the measured ln (K) variance.

4.2. Kalman Filtering

Kalman filtering produces a trend field with more local variation than the fields produced by polynomial regression or hydrofacies delineation, Figures 6 and 7. However, the large-scale trends are weaker and the Kalman filtering field has the lowest ln (K) variance at 1.7, only 40% of measured ln (K) variance. The horizontal correlation length for the estimated field is 108 m, shorter than the 150 m assumed as an input to the method. The scale of hydraulic conductivity variation in the Kalman filtering estimated field is strongly controlled by the assumed input values for correlation lengths and ln (K) variance. By altering these assumed values, estimated fields with a wide array of spatial correlation characteristics could be produced.

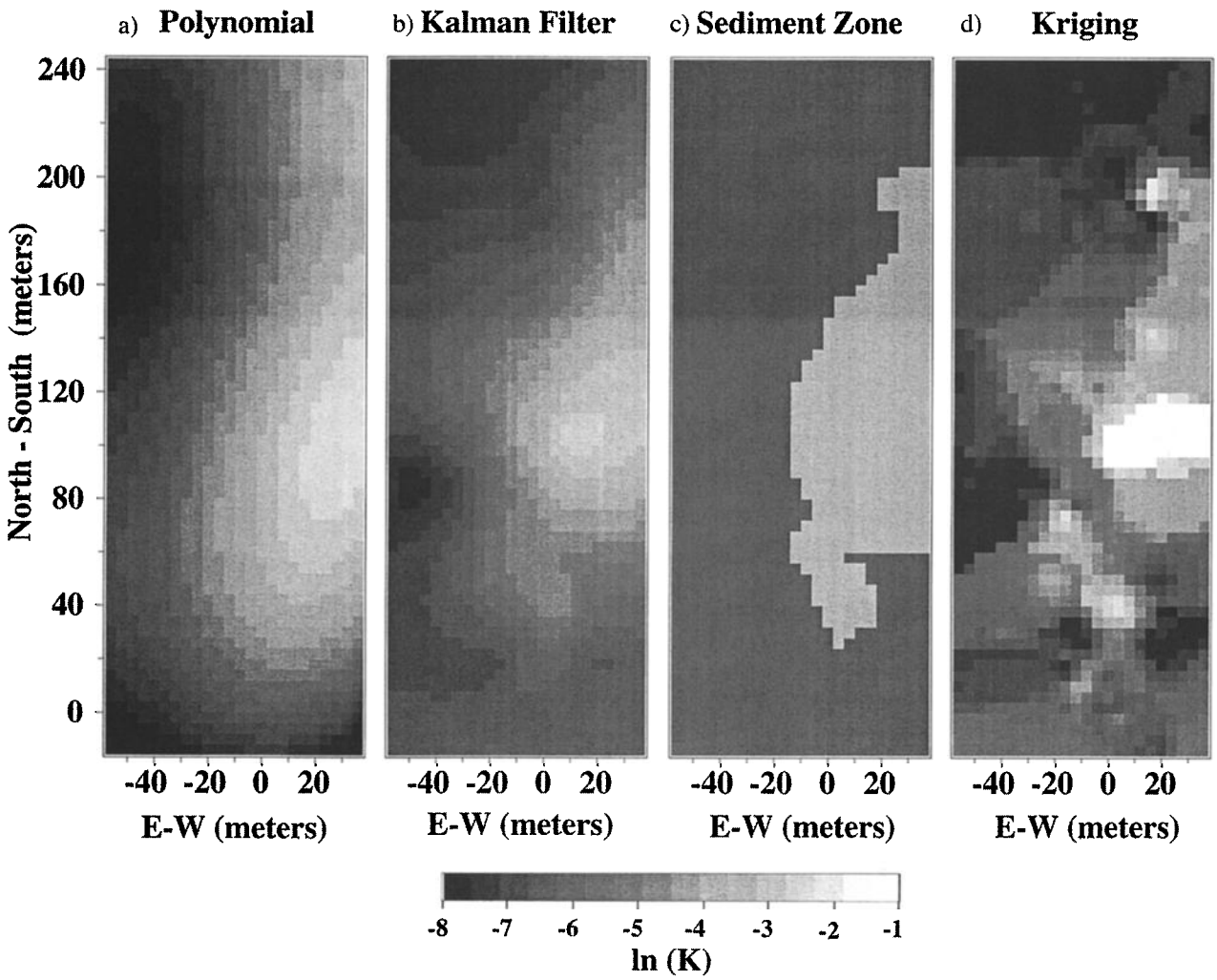

Figure 7. Hydraulic conductivity values, horizontal section at 57.6 m MSL: (a) polynomial regression trend, (b) Kalman filter trend, (c) hydrofacies trend, and (d) Kriged values. Lighter shading indicates higher hydraulic conductivity.

4.3. Hydrofacies Delineation

The geologic architecture method inherently produces a hydraulic conductivity field with sharp discontinuities at contacts of hydrofacies. The ratio of average hydraulic conductivity, based on the flowmeter tests, between the two sediment regions is 24.0 (equation (11)), which is quite close to the ratio of 25 predicted from (2) using average grain size values.

$$\overline{K_{\text{High}}}/\overline{K_{\text{Low}}} = 4.2 \times 10^{-2}/1.75 \times 10^{-3} = 24.0 \qquad (11)$$

The local variability that is excluded by the trend estimation methods can be seen in the kriged field (Figures 6 and 7). If it were possible to show a complete map of the true hydraulic conductivity field, even more local variability would be seen, judging from the observation that ln (K) variance of the kriged field is only 60% of the measured variance.

5. Modeling of Solute Transport

The estimated hydraulic conductivity trends are used as input to a groundwater model to examine how they affect groundwater flow and contaminant transport. Assuming that hydraulic conductivity trends control bulk groundwater flow, if a simulated plume has advective behavior similar to observed plume movement, it suggests that large-scale hydraulic conductivity patterns have been effectively captured by the trend estimation method.

Mean plume displacement is calculated from (12) and (13). Because the Y coordinate axis is aligned with the average groundwater flow direction, only the Y coordinates are included in longitudinal spatial moments calculations. Expressions for spatial moments, (12)–(14) are from *Freyberg* [1986].

$$M_{i,j,k} = n \int\int\int_{-\infty}^{\infty} c(x, y, z) x^i y^j z^k \, dx \, dy \, dz \qquad (12)$$

Mean longitudinal displacement

$$\bar{y} = M_{0,1,0}/M_{0,0,0} \qquad (13)$$

Longitudinal variance

$$\sigma_y^2 = M_{0,2,0}/M_{0,0,0} - (\bar{y})^2 \qquad (14)$$

Dispersive behavior is assessed from temporal changes in second spatial moments of bromide concentrations. Equation (14)

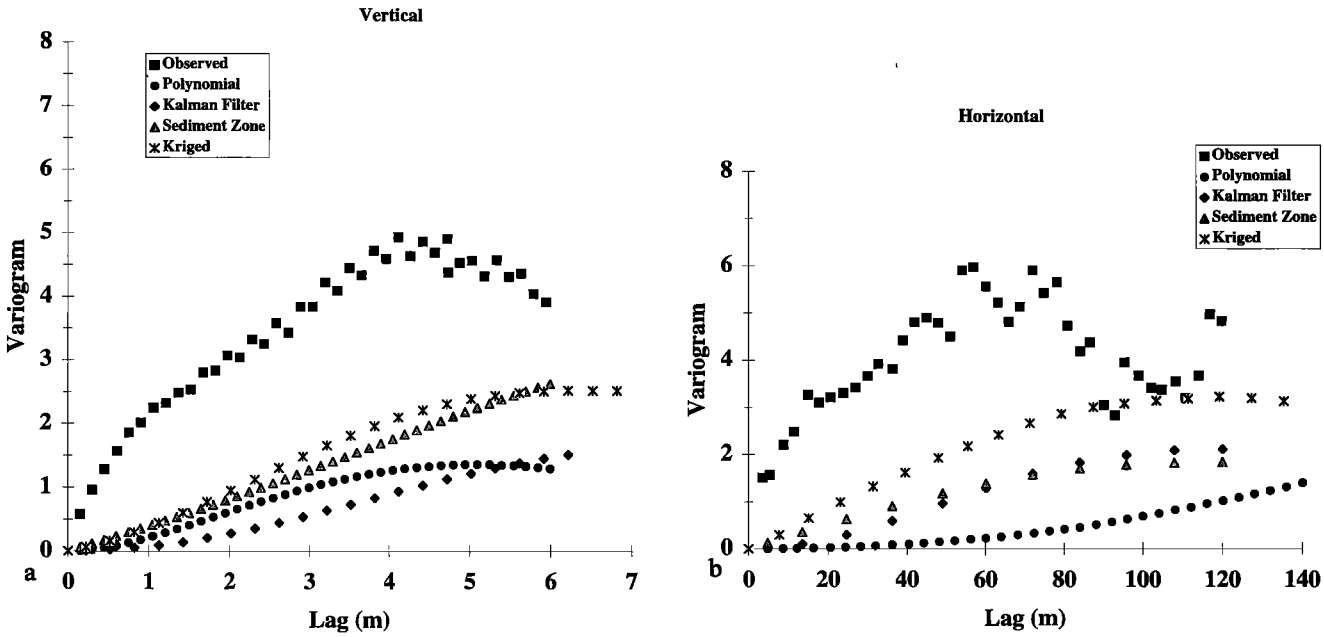

Figure 8. Experimental variograms: (a) vertical variograms, same well pairs only, and (b) horizontal variograms, horizontal isotropy assumed. Observed hydraulic conductivity (flowmeter measurements) variogram values indicated by squares. For each trend method, variograms are calculated from hydraulic conductivity trend values. Polynomial regression is shown with circles; Kalman filtering is shown with diamonds; hydrofacies delineation is shown with triangles; and Kriged is shown with asterisks.

is used to calculate the variance, or second-central moment, of simulated and observed bromide concentrations in the longitudinal direction.

Because small-scale hydraulic conductivity variations are not included in the simulations, it is not expected that simulated plumes should disperse as much as the real plume. An equation for field-scale dispersion of a solute plume, which makes the common assumption that dispersion is caused primarily by variations in flow velocity, is given by *Freyberg* [1986].

$$D_Y = \frac{1}{2}\left(\frac{d\sigma_Y^2}{dt}\right) \tag{15}$$

The spatial moments of the bromide plume injected at Columbus Air Force Base were recreated relatively well by *Adams and Gelhar* [1992] by taking spatial moments of the advection-dispersion equation and preassigning dispersion coefficients and flow velocities that increase linearly in the direction of flow. Despite the good recreation of spatial moments their assumption of an a priori fixed flow field make their model inappropriate for analyzing the effect of hydraulic conductivity on bulk transport behavior, which is the primary concern of this study.

In setting up our groundwater model we only include conditions that would have a strong effect on advective transport behavior. The hydrologic assumptions of the transport model are steady state heads over the duration of the simulation, constant average recharge of 29.2 cm yr^{-1} (obtained by flow model calibration to match observed heads), uniform porosity of 0.35 (following *Adams and Gelhar* [1992]), and constant head boundaries to the north and south and no-flow boundaries to the east and west. The marine sand below the aquifer is assumed to form a no-flow boundary. Partitioning of bromide to solid surfaces and immobile zones is assumed to be instantaneous and linear and a retardation factor of 1.48 is used following *Harvey* [1996, chap. IV]. No dispersion or diffusion coefficients are included. The model domain is 96 by 260 by 10.5 m (X, Y, and Z) with a total of 109,200 nodes, each measuring 4 × 4 × 0.15 m. The 4 m horizontal grid spacing is the largest that can be used while still allowing only one flowmeter well per grid cell. The usual advection equation was solved for head values and flow terms using the program MODFLOW [*McDonald and Harbaugh*, 1988], then particle tracking, implemented with MT3D [*Zheng*, 1992], was used to simulate the bromide transport. Initial concentrations are assigned at the injection well locations to approximate field injection of the bromide solution.

The transport simulations do not attempt to recreate transient behavior of the groundwater system observed at Columbus Air Force Base. The saturated thickness of the surficial aquifer varies seasonally by as much as 40%, and the gradient direction shifts in the horizontal plane seasonally by as much as 40° [*Boggs et al.*, 1990]. Because the observational data have insufficient spatial and temporal resolution to allow detailed description of these transient behaviors over the domain of the plume, we do not attempt to include them in our transport

Table 1. Estimated Hydraulic Conductivity Trend Characteristics

	Mean ln (K)	ln (K) Variance	Correlation Lengths, m	
			λ_v	λ_h
Polynomial regression	−4.7	3.1	4.6	>120
Kalman filtering	−5.4	1.7	>6.0	108
Hydrofacies delineation	−5.5	2.0	>6.0	108
Observed ln (K)	−5.42	4.4	1.4	12.5
Kriging	−5.3	2.6	>6.0	12.0

Table 2. Flow Model Head Analysis

Model Run	Mean Error, m	Maximum Absolute Error, m	Error Variance
Case 1: Elevated Water Table Sampled March 4, 1987 (n = 15)			
Polynomial	−1.49	1.67	0.003
Kalman filter	−1.83	1.90	0.005
Hydrofacies	−1.58	1.67	0.001
Kriging	−1.55	1.66	0.001
Case 2: "Normal" Water Table Sampled April 22, 1987 (n = 14)			
Polynomial	0.31	0.69	0.028
Kalman filter	0.65	0.84	0.013
Hydrofacies	0.56	0.82	0.014
Kriging	0.59	0.83	0.014

model. In addition, the bromide concentrations measured via multiport samplers showed variable mass recoveries that initially totaled 300% of the injected tracer mass and then decreased to ~50% [*Adams and Gelhar*, 1992]. *Harvey* [1996] explained this observed behavior as an increased partitioning of bromide into the immobile flow domain. Our simulations are performed using mass conservative formulations and do not attempt to recreate the fluctuations in measured contaminant mass.

The actual plume showed strong non-Gaussian behavior as can be seen in Figure 3. The maximum observed bromide concentration and the center of bromide mass did not travel far from the injection point, only ~7 and 45 m, respectively, in 503 days, whereas the leading edge of the plume traveled at least 125 m to the farthest monitoring well sampled. Instead of moving as a unit, the plume was patchy, and upper portions of the plume moved into an area of higher hydraulic conductivity and traveled far ahead of the rest of the plume [*Adams and Gelhar*, 1992].

6. Modeling Results

An error analysis was performed that compared steady state modeled heads to measured heads from two sampling events, one performed on March 4, 1987, when the water table was near its highest level, and one performed on April 22, 1987, when the water table was approximately midway between its highest and lowest levels. The error analysis results are shown in Table 2.

Although mean error is large when calculated using the high water level measurements, the error variance is small for all simulated heads. While the largest mean errors indicate that the saturated thickness of the simulated aquifer differs by as much as 18% from the true saturated thickness, the low error variance indicates that local patterns of head variation are reproduced relatively well by the steady state flow model.

As can be seen in Figure 9, the simulated plumes moving in the trend fields are more compact than the actual bromide plume and do not show the main features of the observed plume: high concentrations maintained close to the injection well and a dilute front stretching far ahead of the peak concentrations. The one partial exception to this is the simulated plume moving in the Kalman filter field, which does maintain high concentrations near the injection well. The simulated plume moving in the kriged hydraulic conductivity field, which includes small-scale hydraulic conductivity variations, has small amounts of bromide moving ahead of the peak simulated concentrations but to a much lesser extent than the actual plume.

The observed plume had greater mean horizontal displacement than the simulated trend plumes with the exception of the polynomial trend plume (Figure 10). The higher mean displacement values for the observed plume are caused primarily by the long dilute bromide front. Error in mean horizontal displacement for the simulated trend plumes ranges from −73% to +25%. Of the three simulated trend plumes the sediment zone trend plume most closely matches mean longitudinal displacement of the actual plume. The kriged field

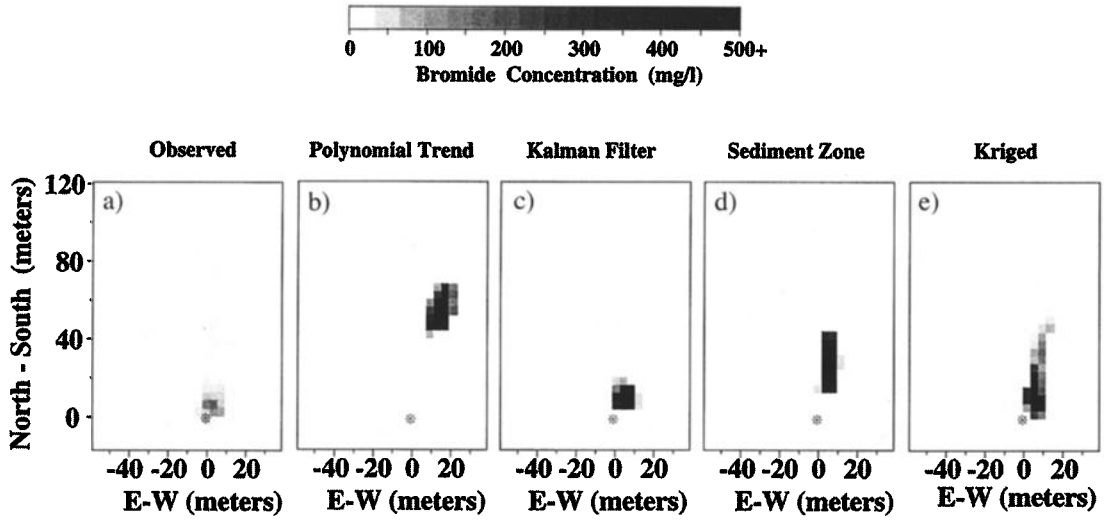

Figure 9. Simulated bromide concentrations (mg L^{-1}) after 503 days of transport, depth-maximum concentrations: (a) observed concentrations, (b) polynomial trend field simulated plume, (c) Kalman filter trend simulated plume, (d) hydrofacies trend simulated plume and (e) kriged field simulated plume. Darker shading indicates higher simulated concentration. Asterisks indicate location of injection wells.

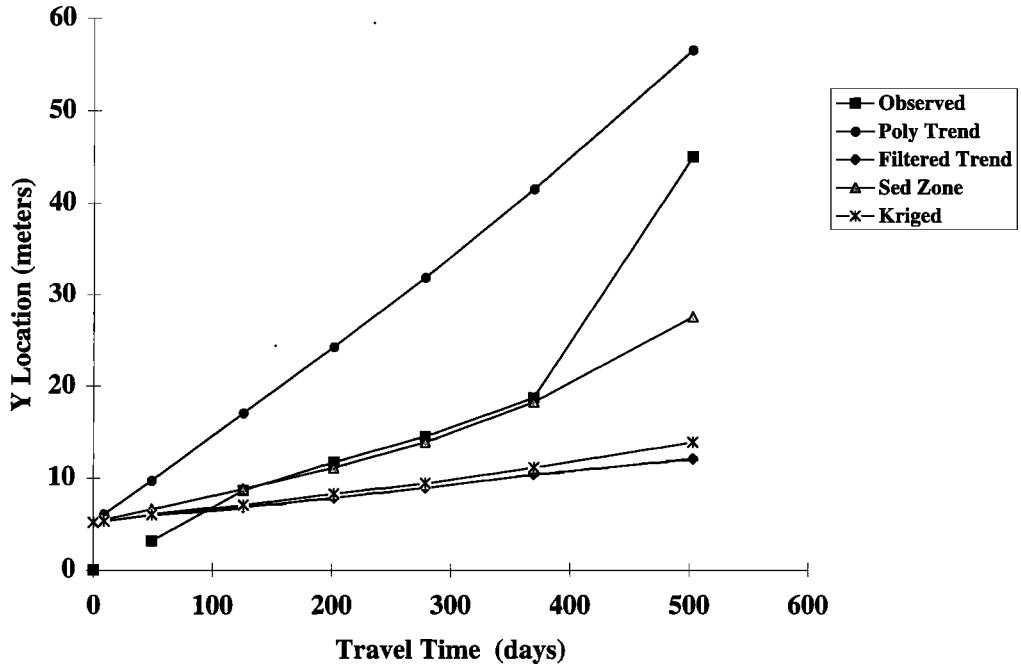

Figure 10. Horizontal center of bromide mass, position in direction of flow: Observed is shown by squares; polynomial regression is shown by circles; Kalman filtering is shown by diamonds; hydrofacies delineation is shown by triangles; and kriging is shown by asterisks. Observed values are from *Adams and Gelhar* [1992, Table 1].

plume also moves more slowly than the actual plume, showing advective behavior that is similar to the sediment zone trend plume.

All of the simulated plumes, like the actual plume, have mean upward displacement (Figure 11). The sediment zone trend plume again comes the closest of the three simulated plumes to matching the advection of the actual plume.

As expected, the simulated plumes, including the plume traveling in the kriged hydraulic conductivity field, all exhibit much less dispersion than the actual plume. If small-scale hy-

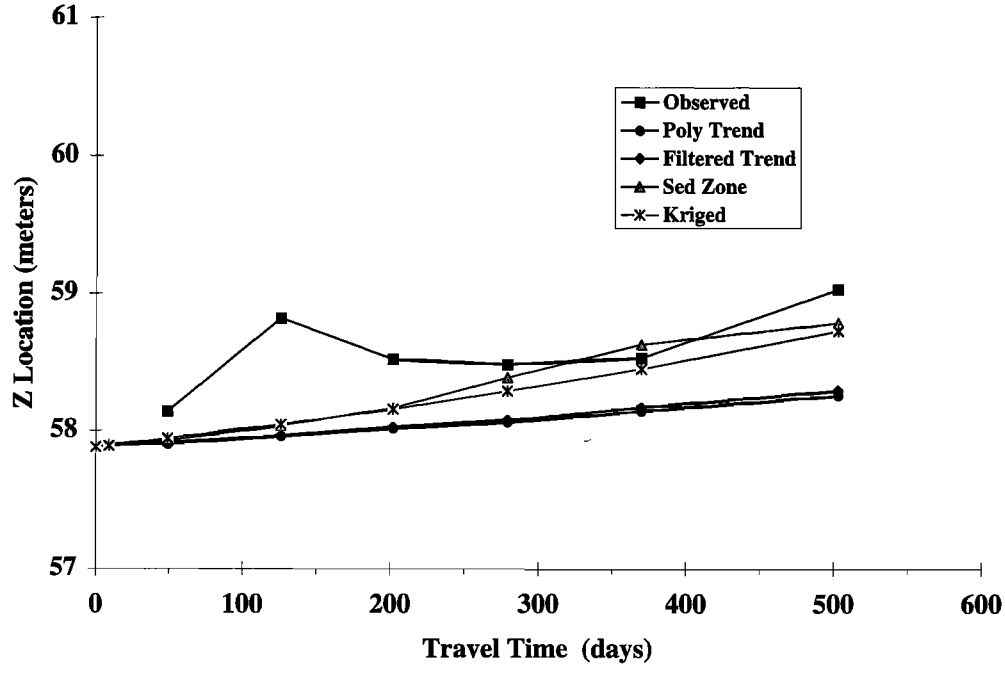

Figure 11. Elevation of the center of bromide mass: Observed is shown by squares; polynomial regression is shown by circles; Kalman filtering is shown by diamonds; hydrofacies delineation is shown by triangles; and Kriging is shown by asterisks. Observed values are from *Adams and Gelhar* [1992, Table 1].

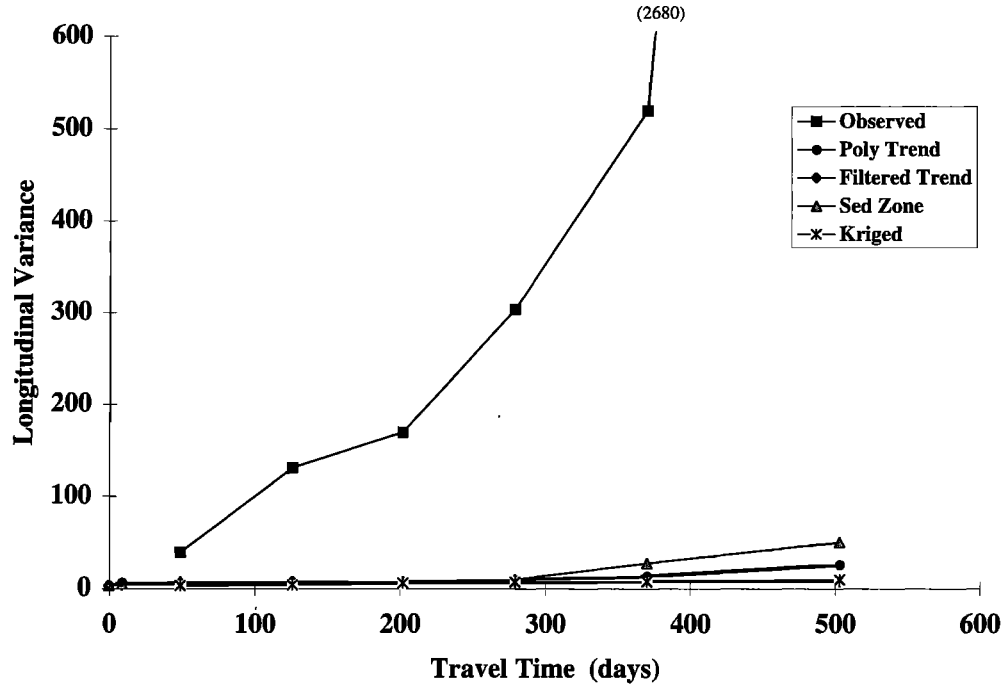

Figure 12. Longitudinal variance of bromide plume. The slope of each plot is twice the dispersion coefficient. Observed is shown by squares; polynomial regression is shown by circles; Kalman filtering is shown by diamonds; hydrofacies delineation is shown by triangles; and Kriging is shown by asterisks. Observed values are from *Adams and Gelhar* [1992, Table 1].

draulic conductivity variations, artificial dispersion, or nonequilibrium partitioning were included in the model, then dispersion in the simulated plumes would be greater. The plots of longitudinal variance with time, whose slopes are twice the dispersion coefficient (equation (15)) show dispersion of the simulated plumes (Figure 12). The little dispersion that is seen in the simulated plumes (~2% of observed dispersion) is caused primarily by hydraulic conductivity variability in the large-scale trend fields. The hydrofacies zone field causes more dispersion than the other two trend fields, despite having a ln (K) variance that is lower.

Some plume spreading is introduced by the numerical implementation of the transport model. To test for numerical dispersion, we performed one simulation in a homogeneous hydraulic conductivity field. It indicated that plume spreading in the hydrofacies zone and kriged hydraulic conductivity fields had a small contribution (~10%) from numerical dispersion but that the lesser plume spreading in the polynomial and Kalman filter trend fields had a significant component of numerical dispersion, 23% and 73%, respectively. In addition to the numerical dispersion, there is numerical dilution caused by spatial averaging of concentrations within grid cells. The introduction of the numerical dispersion and dilution does not change the overall conclusion that large-scale hydraulic conductivity variability present in the trend fields causes only a very small fraction of the total observed dispersion.

7. Discussion

There are significant differences between the hydraulic conductivity fields estimated by the three detrending methods, both in spatial variability and effect on transport. These differences underscore the difficulty of identifying hydraulic conductivity trends in heterogeneous aquifers. Even with nearly 2500 hydraulic conductivity measurements, it is not possible to unambiguously identify large-scale signals controlling advective transport at the Columbus Air Force Base site.

The difficulty in trend identification complicates the use of stochastic equations designed to predict macrodispersion [e.g., *Gelhar and Axness*, 1983] because such equations require a stationary hydraulic conductivity field. If it is not possible to identify and remove major trends, even when an extraordinarily large quantity of subsurface data are available, then the assumptions of these equations cannot be met. The results further indicate that even after removing large-scale trends using common methods, hydraulic conductivity variability remains that can produce a nonstationary velocity field. Small-scale hydraulic conductivity variations that fly under the radar of trend identification methods appear to have significant control over the nonstationary advective plume behavior.

Treating the hydraulic conductivity trend field as an idealized assemblage of two discrete hydrofacies provided a simple means of identifying major hydraulic conductivity patterns. Although the simulated plume moving in the Kalman-filtered field best maintained high concentrations near the injection well, the simulated plume moving in the hydrofacies trend field most closely followed the mean vertical and mean horizontal displacement seen in the actual bromide plume. Despite having more involved methodologies, polynomial regression and Kalman filtering do not lead to more accurate simulations of advective transport. This is important to consider when investigating alluvial aquifers, such as the one at Columbus Air Force Base, where sediment cores and flowmeter measurements show sharp discontinuities in sediment type that may

significantly affect advective transport and that cannot be captured by polynomial regression or Kalman filtering.

The transport simulations do not accurately recreate the non-Gaussian advection of the observed bromide plume. The difference between simulated and actual advective bromide transport is potentially attributable to several factors: (1) failure of the trend estimation methods to capture large-scale trends present in the aquifer, (2) incorrect assignment of parameters model other than hydraulic conductivity in the transport, or (3) local-scale hydraulic conductivity variations exerting significant control over actual plume behavior. Because all of the detrending methods produce fields that like the measured flowmeter values, have hydraulic conductivity increasing north of the injection well, west to east, and with elevation, it is reasonable to conclude that they capture at least the most obvious large-scale patterns of hydraulic conductivity variation. The question of whether transport model parameters other than hydraulic conductivity are assigned incorrectly is more difficult to answer because of the wide variety of potentially important differences between the actual groundwater system and the model system. The seasonal variability of the natural system is ignored in the transport model, but boundary conditions and recharge were chosen to reflect average conditions, and the transport time of 503 days is long enough to average some of the seasonal variability. Although the temporal variability in heads may have a significant effect on dispersive transport, its effect on advective transport should not be large compared to the effect of large-scale hydraulic conductivity variability. The porosity and retardation coefficient are best estimate values from *Adams and Gelhar* [1992] and *Harvey* [1996] and should have spatial variability that is insignificant relative to hydraulic conductivity variability. Although these model parameters may not be assigned correctly, it would be difficult to conceive of reasonable changes to them that would allow the simulated bromide plumes to mimic the strong non-Gaussian behavior seen in the actual plume.

The differences between simulated and actual plumes are therefore probably caused by hydraulic conductivity variations below the scale of flowmeter measurements ($\sim 10^1$ m) that exert significant control over observed plume behavior. Fine-scale layering (10^{-2}–10^{-1} m thickness) is present in the aquifer sediments [*Boggs et al.*, 1990; *Eggleston and Rojstaczer*, 1998] and evidence of fine-scale hydraulic conductivity variations controlling advective behavior is given by the transport simulation in the kriged field. The hydraulic conductivity field produced by kriging includes more small-scale hydraulic conductivity variation than the estimated trend fields, and the simulated plume traveling in the kriged field shows a hint of the observed non-Gaussian transport behavior.

Without identifying the hydraulic conductivity patterns controlling advective transport it is not possible to make accurate predictions of transport. Our results suggest that at the Columbus site, small-scale (<10 m) hydraulic conductivity structures have significant control over bulk transport. Examination of the sediment facies may provide useful information for improving predictions of transport. In heterogeneous alluvial aquifers, prediction of non-Gaussian transport behavior, if it is predictable at all, will apparently require knowledge of fine-scale hydraulic conductivity structures.

Acknowledgments. This work was supported in part by GSA student research grant 5812-96 and by NSF grant EAR-9458376-02. The authors thank the Electric Power Research Institute for supplying the Columbus Air Force Base data.

References

Adams, E. E., and L. W. Gelhar, Field study of dispersion in a heterogeneous aquifer, 2, Spatial moments analysis, *Water Resour. Res.*, *28*, 3293–3307, 1992.

Boggs, J. M., S. C. Young, D. J. Benton, and Y. C. Chung, Hydrogeologic characterization of the MADE site, *Interim Rep. EN-6915*, Electr. Power Res. Inst., Palo Alto, Calif., 1990.

Brannan, J. R., and J. S. Haselow, Compound random field models of multiple scale hydraulic conductivity, *Water Resour. Res.*, *29*, 365–372, 1993.

Cushman, J. H. (Ed.), *Dynamics of Fluids in Hierarchical Porous Media*, 505 pp., Academic, San Diego, Calif., 1990.

Dagan, G., Stochastic modeling of groundwater flow by unconditional and conditional probabilities, 2, The solute transport, *Water Resour. Res.*, *18*, 813–833, 1982.

Dagan, G., Statistical theory of groundwater flow and transport: Pore to laboratory, laboratory to formation, and formation to regional scale, *Water Resour. Res.*, *22*, 120–134, 1986.

Eggleston, J. R., and S. Rojstaczer, Inferring spatial correlation of hydraulic conductivity from sediment cores and outcrops, *Geophys. Res. Lett.*, *25*, 2317–2320, 1998.

Eggleston, J. R., S. A. Rojstaczer, and J. J. Pierce, Identification of hydraulic conductivity structure in sand and gravel aquifers: Cape Cod data set, *Water Resour. Res.*, *32*, 1209–1222, 1996.

Fogg, G. E., Groundwater flow and sand body interconnectedness in a thick multiple aquifer system, *Water Resour. Res.*, *22*, 679–694, 1986.

Freyberg, D. L., A natural gradient experiment on solute transport in a sand aquifer, 2, Spatial moments and the advection and dispersion of nonreactive tracers, *Water Resour. Res.*, *22*, 2031–2046, 1986.

Gelhar, L. W., and C. L. Axness, Three-dimensional stochastic analysis of macrodispersion in aquifers, *Water Resour. Res.*, *19*, 161–180, 1983.

Güven, O. G., F. J. Molz, and J. G. Melville, An analysis of dispersion in a stratified aquifer, *Water Resour. Res.*, *20*, 1337–1354, 1984.

Harvey, C. F., Solute transport in spatially heterogeneous aquifers: Mapping large-scale structures and modeling small-scale effects, Ph.D. thesis, Dep. of Geol. and Environ. Sci., Stanford Univ., Stanford, Calif., 1996.

Hess, K. M., S. H. Wolf, and M. A. Celia, Large-scale natural gradient tracer test in sand and gravel, Cape Cod, Massachusetts, 3, Hydraulic conductivity and calculated macrodispersivities, *Water Resour. Res.*, *28*, 2011–2027, 1992.

Hill, M. C., F. A. D'Agnese, and H. C. Barlebo, Physics, geology, hydrology and effective-value inverse modeling of complex groundwater systems, *Geol. Soc. Am. Abstr. Programs*, A-388, 1996.

Koltermann, C. E., and S. M. Gorelick, Heterogeneity in sedimentary deposits: A review of structure-imitating, process-imitating, and descriptive approaches, *Water Resour. Res.*, *32*, 2617–2658, 1996.

Mallory, M., Hydrogeology of the Southeastern Coastal Plain aquifer system in parts of eastern Mississippi and western Alabama, *U.S. Geol. Surv. Prof. Pap.*, 1410-G, 1993.

McDonald, M. G., and A. W. Harbaugh, A modular three-dimensional finite-difference ground-water flow model, in *U.S. Geological Survey Techniques of Water-Resources Investigations*, vol. 6, chap. A1, 586 pp., U.S. Geol. Surv., Reston, Va., 1988.

Neuman, S. P., Universal scaling of hydraulic conductivities and dispersivities in geologic media, *Water Resour. Res.*, *26*, 1749–1758, 1990.

Rajaram, H., and D. McLaughlin, Identification of large-scale spatial trends in hydrologic data, *Water Resour. Res.*, *26*, 2411–2423, 1990.

Rehfeldt, K. R., P. Hufschmied, L. W. Gelhar, and M. E. Schaefer, Measuring hydraulic conductivity with the borehole flowmeter, *Top. Rep. EN-6511*, Electr. Power Res. Inst., Palo Alto, Calif., 1989.

Rehfeldt, K. R., J. M. Boggs, and L. W. Gelhar, Field study of dispersion in a heterogeneous aquifer, 3, Geostatistical analysis of hydraulic conductivity, *Water Resour. Res.*, *28*, 3309–3324, 1992.

Russo, D., and W. A. Jury, A theoretical study of the estimation of the correlation scale in spatially variable fields, 1, Stationary fields, *Water Resour. Res.*, *23*, 1257–1268, 1987a.

Russo, D., and W. A. Jury, A theoretical study of the estimation of the correlation scale in spatially variable fields, 2, Nonstationary fields, *Water Resour. Res.*, *23*, 1269–1279, 1987b.

Scheibe, T. D., and C. R. Cole, Non-Gaussian particle tracking: Application to scaling of transport processes in heterogeneous porous media, *Water Resour. Res.*, *30*, 2027–2039, 1994.

Scheibe, T. D., and D. L. Freyberg, Use of sedimentological information for geometric simulation of natural porous media structure, *Water Resour. Res.*, *31*, 3259–3270, 1995.

Sudicky, E. A., A natural gradient experiment on solute transport in a sand aquifer: Spatial variability of hydraulic conductivity and its role in the dispersion process, *Water Resour. Res.*, *22*, 2069–2082, 1986.

Webb, E. K., and M. P. Anderson, Simulation of preferential flow in three-dimensional, heterogeneous conductivity fields with realistic internal architecture, *Water Resour. Res.*, *32*, 533–545, 1996.

Weber, K. J., How heterogeneity affects oil recovery, in *Reservoir Characterization*, edited by L. W. Lake and H. B. Carroll, pp. 487–544, Academic, San Diego, Calif., 1986.

Young, S. C., J. Herweijer, and D. J. Benton, Geostatistical evaluation of a three-dimensional hydraulic conductivity field in an alluvial terrace aquifer, in *Fifth Canadian/American Conference on Hydrogeology*, edited by S. Bachu, pp. 116–135, Natl. Water Well Assoc., Dublin, Ohio, September, 1990.

Zheng, C., MT3D: A modular three-dimensional transport model, in *Documentation and User's Guide*, 2nd ed., S. S. Papadopulos, Bethesda, Md., 1992.

J. Eggleston and S. Rojstaczer, Center for Hydrologic Science, Duke University, Box 90230, Durham, NC 27708-0230. (e-mail: jre4@acpub.duke.edu)

(Received November 17, 1997; revised April 28, 1998; accepted May 1, 1998.)